Computer Assisted Mechanics and Engineering Sciences, 8: 543–556, 2001.

Coupling generalized FC model to meshless EFG method for crack growth analysis in quasi-brittle materials

Czesław Cichoń and Jan Jaśkowiec
Institute of Computer Methods in Civil Engineering, Cracow University of Technology, ul. Warszawska 24, 31-155 Kraków, Poland

(Received February 14, 2000)

In the paper a crack growth analysis in quasi brittle materials in plane stress state coupling the Fictitious Crack model to meshless Element-Free Galerkin method is presented. The FC model has been generalized and as a result a uniform algorithm of the analysis of crack propagation, which is a combination of elementary states mode I and mode II has been prepared. The problem is nonlinear because the traction forces contain, besides external loads, cohesive forces on the boundaries of the crack which depend on the actual state of the displacement field. The efficiency of the method has been tested on two standard examples.

1. Introduction

Design of civil engineering structures often needs special analysis of crack propagation to ensure its safety over a long lifetime. Such regulations take place for example when the structure is made from quasi-brittle materials like concrete or different kind of refractory ceramics [28]. In solid mechanics there is a large number of methods of analysis of cracked structures, however the crack growth is generally based on damage mechanics or fracture mechanics. In damage mechanics the continuity of material is assumed and the response of the material with cracks is modeled with the help of an equivalent homogeneous material [20, 26]. In fracture mechanics, discontinuity of the cracked material is taken into account [18].

In the paper, the nonlinear fracture mechanics is explored and crack growth analysis of a structure up to failure is performed using ideas of the fictitious crack model (FC model) originally developed by Hilleborg et al. [16]. This model is generalized on the stress state cases which are combinations of elementary states, called opening mode I and sliding mode II , and is based on the idea of replacing the scalar measure of the crack opening displacement with relative crack displacement vector. Such extension of Hilleborg's model is important in the discrete analysis of the crack propagation in concrete and usually needs formulation of more complex form of the cohesive law, see [1, 29]. Separate research problems is the occurrence of pure mode II and dependence of the mixed-mode fracture on the so-called size effect. These questions are still open and under experimental and numerical investigations [3, 14, 17, 23].

An effective application of this method to the analysis of more complex structures needs a numerical (approximated) method of analysis. Up to now, the problem of the mixed-mode fracture has mainly been considered in the context of the finite element method (FEM) and theory of plasticity. Such approach is however not so productive if the crack propagates in an a priori unknown direction. A standard approach is, in that case, remeshing in the vicinity of the crack tip [30].

The crack in concrete was analysed in [24] and the initial yield surface expressed with the help of is introduced and softening is defined in terms of traction against relative crack displacements. Implementation of a plasticity-type constitutive law to the mixed-mode fracture was also proposed in [8] where interface finite elements were used. An interesting numerical model, limited however to mode I crack growth analysis only, was presented in [9] where the effective stiffness matrix, which is

a difference between the stiffness matrix and the softening matrix, was introduced and the problem was solved iteratively.

It should be noted that an alternative to the Hilleborg's discrete model can stand the crack band model (CB model), developed by Bažant and Oh [2] where it is assumed that crack formation in the concrete occurs in the form of a blunt smeared crack band. This model is practically limited to mode I cracks and its extension needs introducing a high number of parameters, thus completely losing computational simplicity which is the most attractive fashion of the CB model [13].

In recent years there have been intensively developed computer methods to the analysis of boundary-value problems based on nodes rather than on elements and known under the common name of meshless methods. Some of these methods have been known for at least 25 years but only recently they have found effective applications [4, 19, 21, 22, 25].

Among the meshless methods probably the most popular and useful in fracture mechanics is the so-called Element-Free Galerkin method (EFG method) developed mainly by Belytchko and co-workers [6, 7]. This method links the idea of local approximation based on the weighted moving least square method with the well known Galerkin method.

In the paper, the generalized FC model is coupled to the EFG method and the uniform algorithm of the crack growth analysis is presented. The extension of this work will be coupling the EFG method to the FEM. Such coupling was originally proposed by Hegen in [15] where Linear Elastic Fracture Mechanics (LEFM) was used to the simulation of quasi-static crack propagation in brittle materials.

In the present paper the following assumptions are adopted. The structure is in the plane stress state. The material of continuum is linearly elastic and displacements and their gradients are small. External load is static and proportional to a one parameter.

The paper is organized as follows. In Section 2 a short description of the weighted moving least square approximation is presented. Basic equations of the EFG method are derived in Section 3. In Section 4 generalized FC model is derived and the algorithm of solution is presented in Section 5. The paper is closed with two examples of crack propagation in concrete beams and some conclusions are included.

2. Weighted moving least square approximation

Let us assume that function $u(x)$, defined on a plane domain Ω, is approximated by function u^h given by

$$u^h(\mathbf{x}) = \mathbf{p}(\mathbf{x})^T \mathbf{a}(\mathbf{x}) \tag{1}$$

where $\mathbf{x}$ contains spatial coordinates, $\mathbf{p}(\mathbf{x})$ is a vector of base functions and $\mathbf{a}(\mathbf{x})$ is a vector of unknown coefficients.

Vector $\mathbf{a}(\mathbf{x})$ can be obtained by minimizing the weighted moving least squares sum I that relates u^h to u_i at nodes $\mathbf{x}_i$,

$$I(\mathbf{x}) = \sum_{i=1}^{n} w(\|\mathbf{x} - \mathbf{x}_i\|) \left[\mathbf{p}(\mathbf{x}_i)\, \mathbf{a}(\mathbf{x}) - u_i\right]^2, \tag{2}$$

where $w(\mathbf{x} - \mathbf{x}_i)$ is the weight function associated with node i and n is the number of nodes. Minimization of (2) with respect to $\mathbf{a}(\mathbf{x})$ yields

$$\mathbf{a}(\mathbf{x}) = \mathbf{A}^{-1}(\mathbf{x})\, \mathbf{C}(\mathbf{x})\, \mathbf{u} \tag{3}$$

where

$$\mathbf{A}(\mathbf{x}) = \mathbf{P}\mathbf{W}(\mathbf{x})\mathbf{P}^T, \qquad \mathbf{C}(\mathbf{x}) = \mathbf{P}\mathbf{W}(\mathbf{x}) \tag{4}$$

and

$$\mathbf{P} = [\mathbf{p}(\mathbf{x}_1), \mathbf{p}(\mathbf{x}_2), \ldots, \mathbf{p}(\mathbf{x}_n)], \qquad \mathbf{W}(\mathbf{x}) = \operatorname{diag}[w(r_1), w(r_2), \ldots, w(r_n)], \tag{5}$$

with weight functions $w(r_i)$, $r_i = \|\mathbf{x} - \mathbf{x}_i\|$, $i = 1, \ldots, n$.

The weight function has the compact support also called the domain of influence of node i in such a way that weight function w is zero outside the domain of influence and $w \geq 0$ inside the domain of influence.

Substitution of (3) into (1) gives

$$u^h(\mathbf{x}) = \mathbf{N}(\mathbf{x})\,\mathbf{u} \tag{6}$$

with the shape functions $\mathbf{N}$ defined as

$$\mathbf{N}(\mathbf{x}) = \mathbf{p}(\mathbf{x})^T\,\mathbf{A}^{-1}(\mathbf{x})\,\mathbf{C}(\mathbf{x})\,. \tag{7}$$

In the following shape functions expressed by formula (7) will be applied to EFG method. In the context of this method it must be stressed that opposite to finite element shape functions, EFG shape functions do not have the selective property, i.e. $N_i(\mathbf{x}_j) \neq \delta_{ij}$ with δ_{ij} the Kronecker delta. The second problem is connected with calculations of the derivatives of the shape functions, which is rather a time consuming numerical operation [5].

In the paper, the derivatives of shape functions are computed in the standard way using the formula

$$\frac{\partial \mathbf{N}(\mathbf{x})}{\partial x_i} = \frac{\partial \mathbf{p}(\mathbf{x})^T}{\partial x_i}\,\mathbf{A}^{-1}(\mathbf{x})\,\mathbf{C}(\mathbf{x}) + \mathbf{p}(\mathbf{x})\,\frac{\partial \mathbf{A}^{-1}(\mathbf{x})}{\partial x_i}\,\mathbf{C}(\mathbf{x}) + \mathbf{p}(\mathbf{x})\,\mathbf{A}^{-1}(\mathbf{x})\,\frac{\partial \mathbf{C}(\mathbf{x})}{\partial x_i} \tag{8}$$

with $\dfrac{\partial \mathbf{A}^{-1}(\mathbf{x})}{\partial x_i}$ computed by

$$\frac{\partial \mathbf{A}^{-1}(\mathbf{x})}{\partial x_i} = -\mathbf{A}^{-1}(\mathbf{x})\,\frac{\partial \mathbf{A}(\mathbf{x})}{\partial x_i}\,\mathbf{A}^{-1}(\mathbf{x})\,. \tag{9}$$

Finally, for the unique identification of crack discretization it is necessary to determine the position of nodes in relation to crack.

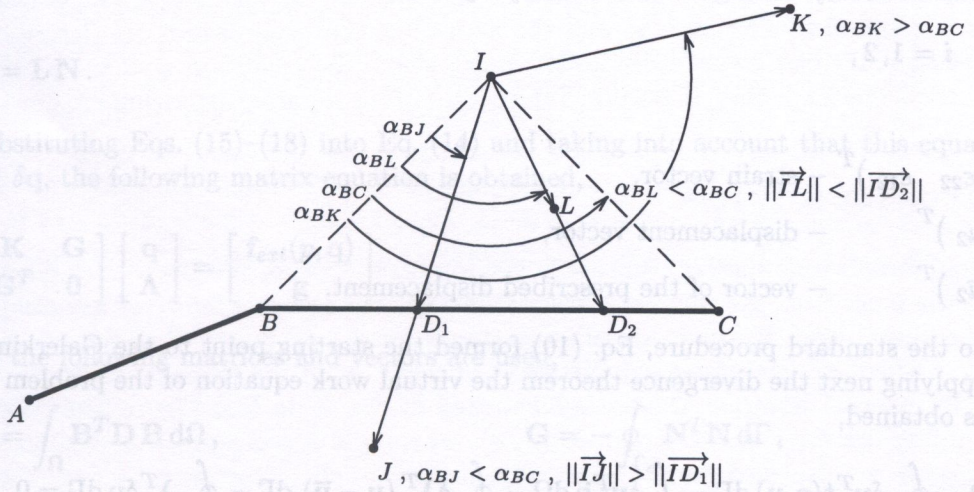

Fig. 1. Determination of the position of a node in relation to crack

Let us assume that the crack is made up of line segments $\ldots A{-}B{-}C$, where C is the crack tip, and I is the integration point and J, K, L are nodes, see Fig. 1. To distinguish the position of the node in relation to the crack segment a simple but effective method is proposed. For example, as shown in Fig. 1, on the base of known values of angles α_{BJ}, α_{BC} and lengths of vectors $\|\overrightarrow{IJ}\|$, $\|\overrightarrow{ID}\|$ it can be concluded that node J is on the opposite side of the crack segment to point I. Points L and K are, however, on the same side of the crack segment as point I.

Specification of the position of nodes in relation to the crack is necessary for the proper description of displacement discontinuities over the crack. Different methods of introducing the discontinuities into meshless approximations are well known in literature. In the paper so-called diffraction method has been used. The main idea of this method is to treat the line of discontinuity as opaque but to evaluate the "distance" r_i between two nodes by a path which passes around the corner of the discontinuity [5].

3. Basic equations of the EFG method

The equilibrium equations on a plane domain Ω has the form

$$\mathbf{L}^T\boldsymbol{\sigma} + \mathbf{b} = \mathbf{0} \tag{10}$$

with the natural boundary conditions on boundary Γ_n of Ω,

$$\sigma_{ij} n_i = \bar{t}_j\,, \qquad i,j = 1,2\,, \tag{11}$$

where

$\boldsymbol{\sigma} = \left(\sigma_{11} \quad \sigma_{22} \quad \sigma_{12}\right)^T$ – stress vector,

$\mathbf{b} = \left(b_1 \quad b_2\right)^T$ – body forces vector,

$\mathbf{n} = \left(n_1 \quad n_2\right)^T$ – vector of the outward normal to Γ_n,

$\bar{\mathbf{t}} = \left(\bar{t}_1 \quad \bar{t}_2\right)^T$ – vector of the prescribed tractions forces.

Using the matrix of differential operators $\mathbf{L}$, the geometrical equations can be written as

$$\boldsymbol{\varepsilon} = \mathbf{L}\,\mathbf{u} \tag{12}$$

with the essential boundary conditions on boundary Γ_e of Ω

$$u_i = \bar{u}_i\,, \qquad i = 1,2\,, \tag{13}$$

where

$\boldsymbol{\varepsilon} = \left(\varepsilon_{11} \quad \varepsilon_{22} \quad \varepsilon_{12}\right)^T$ – strain vector,

$\mathbf{u} = \left(u_1 \quad u_2\right)^T$ – displacement vector,

$\bar{\mathbf{u}} = \left(\bar{u}_1 \quad \bar{u}_2\right)^T$ – vector of the prescribed displacement.

According to the standard procedure, Eq. (10) formed the starting point to the Galerkin weak formulation. Applying next the divergence theorem the virtual work equation of the problem under consideration is obtained,

$$\int_\Omega \delta\boldsymbol{\varepsilon}^T\boldsymbol{\sigma}\,\mathrm{d}\Omega - \oint_{\Gamma_n} \delta\mathbf{u}^T\mathbf{t}(p,\mathbf{u})\,\mathrm{d}\Gamma - \int_\Omega \delta\mathbf{u}^T\mathbf{b}\,\mathrm{d}\Omega - \oint_{\Gamma_e} \delta\boldsymbol{\lambda}^T(\mathbf{u}-\bar{\mathbf{u}})\,\mathrm{d}\Gamma - \oint_{\Gamma_e} \boldsymbol{\lambda}^T\delta\mathbf{u}\,\mathrm{d}\Gamma = 0\,. \tag{14}$$

To overcome the problem that the method lacks the selectivity property the Lagrange multipliers method has been used. Other methods are also possible and derived in literature [4]. It must be noted that the above equation is nonlinear because traction forces $\mathbf{t}$ contain, besides external loads, cohesive forces on the boundaries of the crack which depends on the actual state of the displacement field $\mathbf{u}$ (see Section 4). This fact has been stressed in Eq. (14) by writing $\mathbf{t} = \mathbf{t}(p, \mathbf{u})$, where p is the load parameter. The next problem is that in the process of loading, bothe geometry of the crack and, as a result, the boundary Γ_n, have changed.

In the following the continuous problem is changed into discretized one. The approximation of the displacement has the form:

$$\mathbf{u} = \begin{bmatrix} u_1 \\ u_2 \end{bmatrix} = \mathbf{N}\mathbf{q}, \tag{15}$$

where $\mathbf{N} = [\, \mathbf{N}_{u_1} \quad \mathbf{N}_{u_2} \,]$ – shape functions matrix.

The approximation of Lagrange multipliers can be written as:

$$\boldsymbol{\lambda} = \mathbf{N}_\lambda \boldsymbol{\Lambda}, \tag{16}$$

where

$\boldsymbol{\Lambda}$ – vector of the discretized Lagrange multipliers,

$\mathbf{N}_\lambda$ – part of matrix $\mathbf{N}$ to which the nodes of Γ_e apply.

It is assumed that the material of continuum is elastic and the constitutive relation is of the form:

$$\boldsymbol{\sigma} = \mathbf{D}\boldsymbol{\varepsilon}, \tag{17}$$

where $\mathbf{D}$ – constitutive stiffness matrix.

The displacements and their gradients are small, which enables us to write the geometrical equation in the discretized form as

$$\boldsymbol{\varepsilon} = \mathbf{B}\mathbf{q}, \tag{18}$$

where

$$\mathbf{B} = \mathbf{L}\mathbf{N}. \tag{19}$$

Substituting Eqs. (15)–(18) into Eq. (14) and taking into account that this equation must hold for all $\delta\mathbf{q}$, the following matrix equation is obtained,

$$\begin{bmatrix} \mathbf{K} & \mathbf{G} \\ \mathbf{G}^T & \mathbf{0} \end{bmatrix} \begin{bmatrix} \mathbf{q} \\ \boldsymbol{\Lambda} \end{bmatrix} = \begin{bmatrix} \mathbf{f}_{ext}(p, \mathbf{q}) \\ \mathbf{g} \end{bmatrix} \tag{20}$$

where the following matrices and vectors are used,

$$\mathbf{K} = \int_\Omega \mathbf{B}^T \mathbf{D}\, \mathbf{B}\, \mathrm{d}\Omega, \qquad \mathbf{G} = -\oint_{\Gamma_e} \mathbf{N}^T \mathbf{N}\, \mathrm{d}\Gamma, \tag{21}$$

$$\mathbf{f}_{ext} = \oint_{\Gamma_u} \mathbf{N}^T \mathbf{t}(p, \mathbf{q})\, \mathrm{d}\Gamma + \int_\Omega \mathbf{N}^T \mathbf{b}\, \mathrm{d}\Omega, \qquad \mathbf{g} = \oint_{\Gamma_e} \mathbf{N}_\lambda^T \bar{\mathbf{u}}\, \mathrm{d}\Gamma. \tag{22}$$

4. Generalized FC model of the crack growth

In this Section the idea of Hilleborg's fictitious crack model is extended on the case in which the crack growth is a combination of opening mode I and sliding mode II . Consequently , instead of the scalar measure of crack opening, the crack opening vector $\vec{w}$ is introduced, Fig. 2a. This vector describes the direction in which the cohesive forces are applied and its length is the measure of crack opening, $w = \|\vec{w}\|$. In Fig. 2a $\vec{u_A}$ and $\vec{u_B}$ are displacement vectors and A, B and A_1 , B_2 are points on the fictitious crack faces before and after deformation, respectively. The distribution of cohesive stresses is shown in Fig. 2b and the function of the crack-stress opening $\sigma = f(w)$ is shown in Fig. 2c.

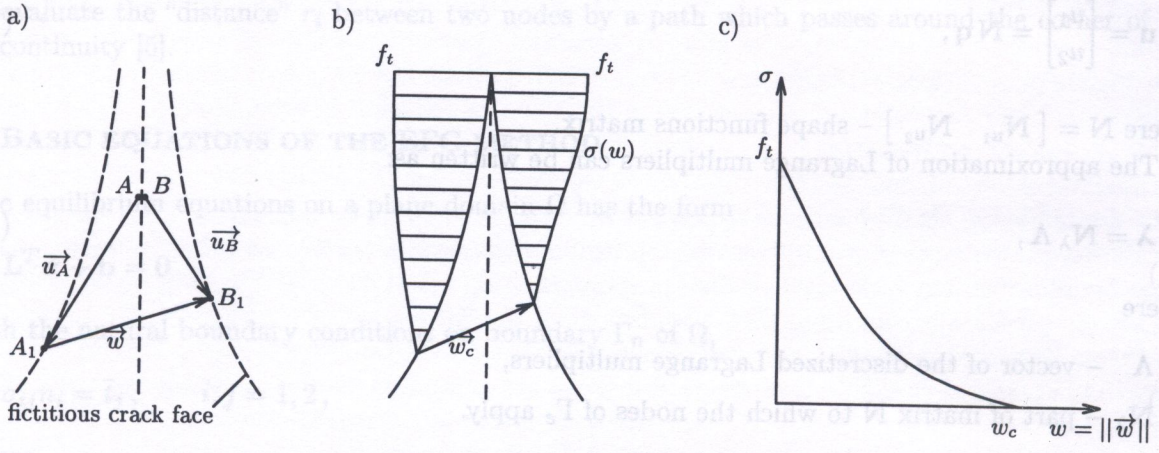

Fig. 2. (a) definition of a crack opening vector $\vec{w}$, (b) distribution of cohesive stresses, (c) stress crack opening curve

The crack growth is analysed under the assumption that the crack initiates at a point where the maximal principal stress reaches the tensile strength f_t .

The stress-crack opening curves can in general be described by two main parameters: (1) the area under the complete curve, representing fracture energy G_f^H, and (2) the initial shape of the curve which may be characterized by the area under the initial tangent representing initial fracture energy G_f^i . The shape of curve $f(w)$ has a minor effect on the predicted fracture behaviour of structures and can hardly be experimentally determined without ambiguity [11].

As stated in Section 3, in numerical computations the cohesive stresses acting across the fracture zone are replaced by nodal forces and these forces are components of vector $\mathbf{f_{ext}}$. As a result of the iterative process the new external load and the actual fracture zone length are described. In consequence the real crack can be extended to the point where the condition $w = w_c$ is fulfilled, where w_c is the critical crack opening. In Section 5 the details of the iterative algorithm are described.

5. Algorithm of the solution

Solution of the equilibrium equation (20) is made in two iterative loops for the given crack geometry, $k = 1, \ldots, \overline{k}$. In the inner loop, the cohesive forces across the boundaries of the crack are computed for the constant external load. In the external loop, the external load is described for which $\sigma = \max(\sigma_1, \sigma_2) = f_t$, where σ_1 , σ_2 are principal stresses at point A_k of the foreseen direction of the crack growth. This external iterative process is illustrated in Fig. 3. In this Figure, the solid line represents the equilibrium path of the structure (p, q), where q is a representative displacement. The equilibrium path is calculated for the changed geometry of the structure as a result of the crack growth. Point S_k on the equilibrium path is calculated using bisection method, $j = 1, \ldots, \overline{j}$ (dashed line in Fig. 3).

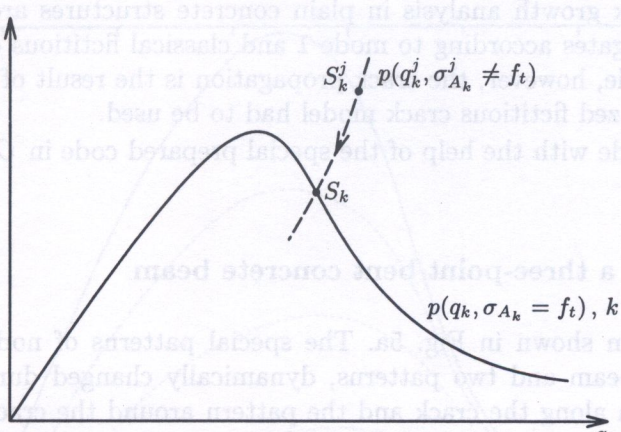

Fig. 3. External equilibrium iteration

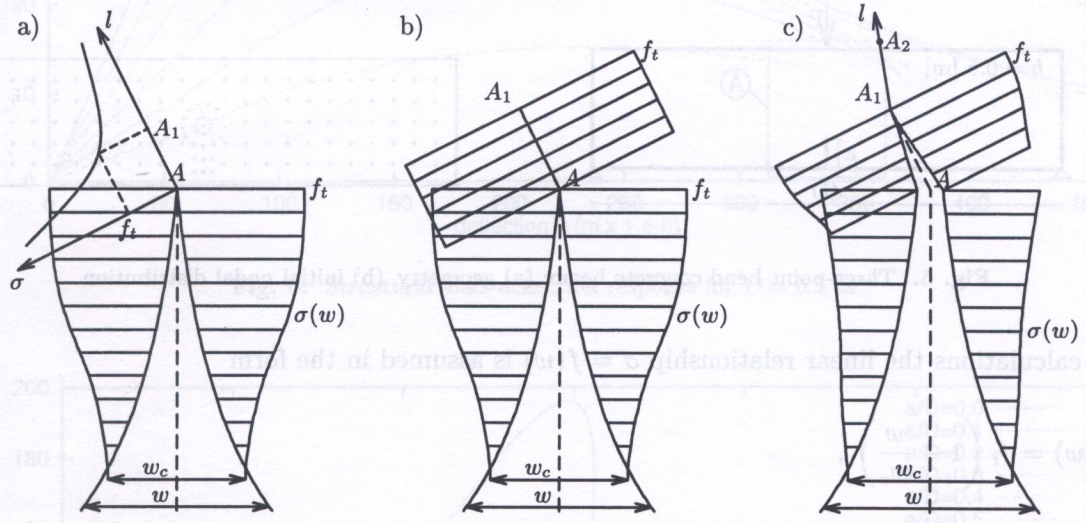

Fig. 4. Three steps of the internal equilibrium iteration: (a) equilibrium of the external loads with cohesive forces, (b) initial distribution of cohesive stresses, (c) final distribution of cohesive stresses

In Fig. 4a, the equilibrium of the external load with cohesive forces at the end of the external loop is shown with the condition $\max(\sigma_1, \sigma_2) = f_t$ at point A_1. The direction of crack propagation l is described by the principal axis of the smaller principal stress, computed at point A. In the next step discontinuity of the crack on the sector line A–A_1 is introduced and the initial distribution of stresses $\sigma = f_t$ is assumed, Fig. 4b. In the result of the iterative process the actual distribution of cohesive stresses is calculated, Fig. 4c. The subsequent point A_2 along direction l, described by the principal axis of the smaller stress at point A_1, is also chosen. As a result of the iterative process, the new equilibrium state is computed for which the condition $\max(\sigma_1, \sigma_2) = f_t$ at the point A_2 is fulfilled.

6. Examples

The method of analysis presented in the paper has been verified on some examples of the crack growth analysis of structures made from different quasi-brittle materials. In [10] the crack growth in the refractory material called Teoxit was investigated.

Two examples of the crack growth analysis in plain concrete structures are presented. In the first example the crack propagates according to mode I and classical fictitious crack model can be applied. In the second example, however, the crack propagation is the result of mixture of mode I and mode II and the generalized fictitious crack model had to be used.

All computations were made with the help of the special prepared code in *C++*.

6.1. Crack propagation in a three-point bent concrete beam

The three-point bent beam in shown in Fig. 5a. The special patterns of nodes were generated: the regular pattern for the beam and two patterns, dynamically changed during propagation of the crack, namely the pattern along the crack and the pattern around the crack tip, Fig. 5b. The following material parameters are assumed: $E = 30$ GPa, $\nu = 0.3$, $ft = 1.0$ MPa.

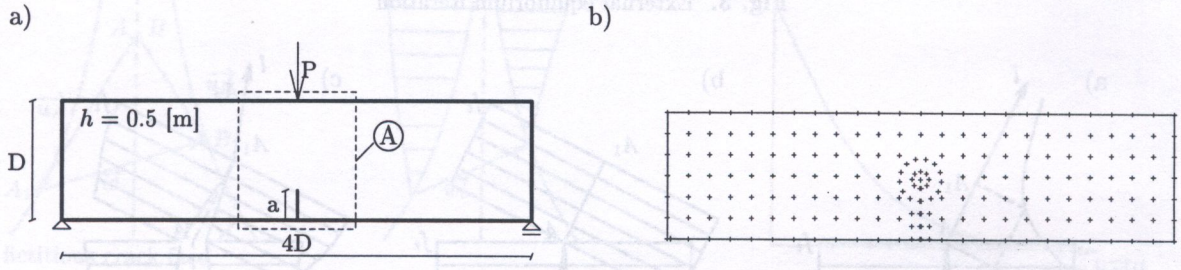

Fig. 5. Three-point bend concrete beam; (a) geometry, (b) initial nodal distribution

In calculations the linear relationship $\sigma = f(w)$ is assumed in the form

$$\sigma(w) = f_t \left(1 - \frac{w}{w_c}\right), \tag{23}$$

where $w_c = 0.1$ mm.

It is also assumed that the vector of basic functions $\mathbf{p}(\mathbf{x})$ is

$$\mathbf{p}(\mathbf{x}) = \begin{pmatrix} 1 & x & y & xy \end{pmatrix}^T, \tag{24}$$

and the weight function has been assumed in the form

$$w(r) = \exp\left(-\left(\frac{r}{\beta}\right)^2\right) \qquad \text{where} \qquad \beta = 1.3/\rho \tag{25}$$

and ρ is the density function of nodes, defined for each individual pattern [31].

In the example the effect of the dimensional scale on the brittleness of the beam is analysed, Figs. 6–9. From these pictures it is seen that the brittleness considerably increases as the beam depth D increases, with a/D constant. As well known it is a result of redistribution of stresses and localization of damage in the process zone during the stable growth of the crack and can be only taken into account with the help of the FC model. The effect of this localization is the vanishing influence on the rest of the structure, rendering a deviation from the LEFM size effect.

In Fig. 10 the picture of the deformed part Ⓐ of the beam is schematically shown. It is seen that the deformation for the cracked beam is adequate to the opening mode I .

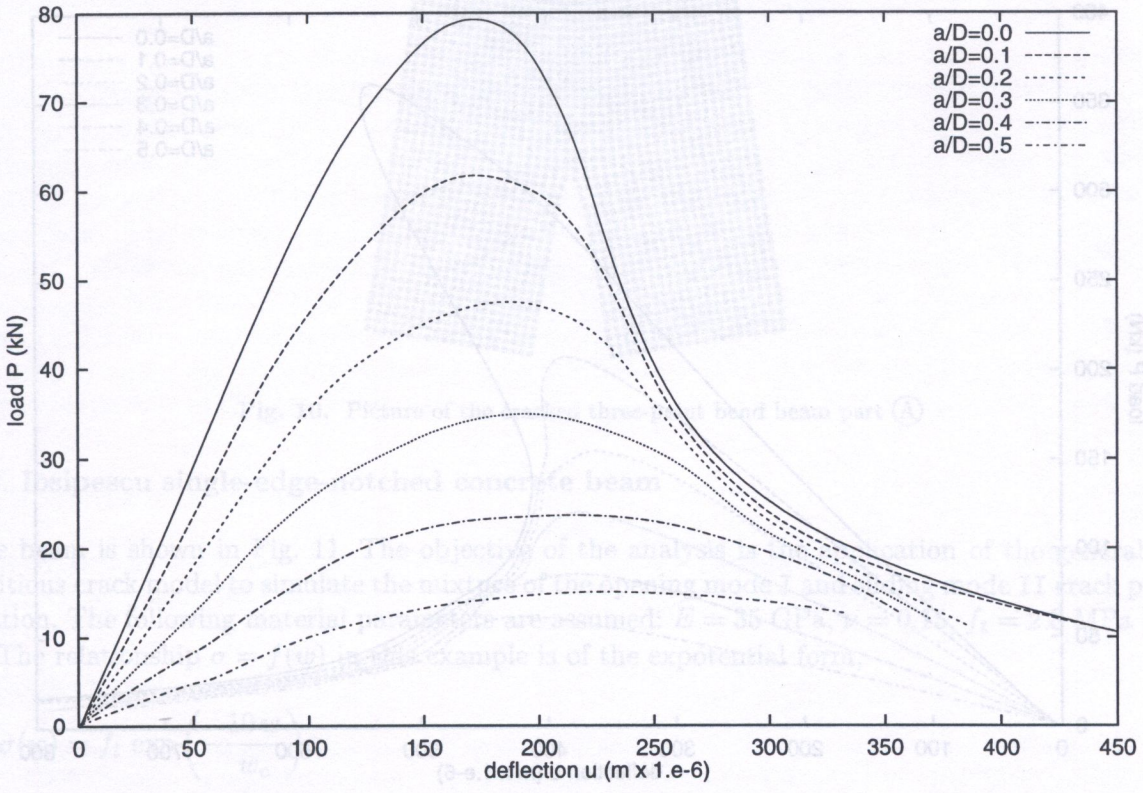

Fig. 6. Structural load–deflection response for $D = 0.8$ m

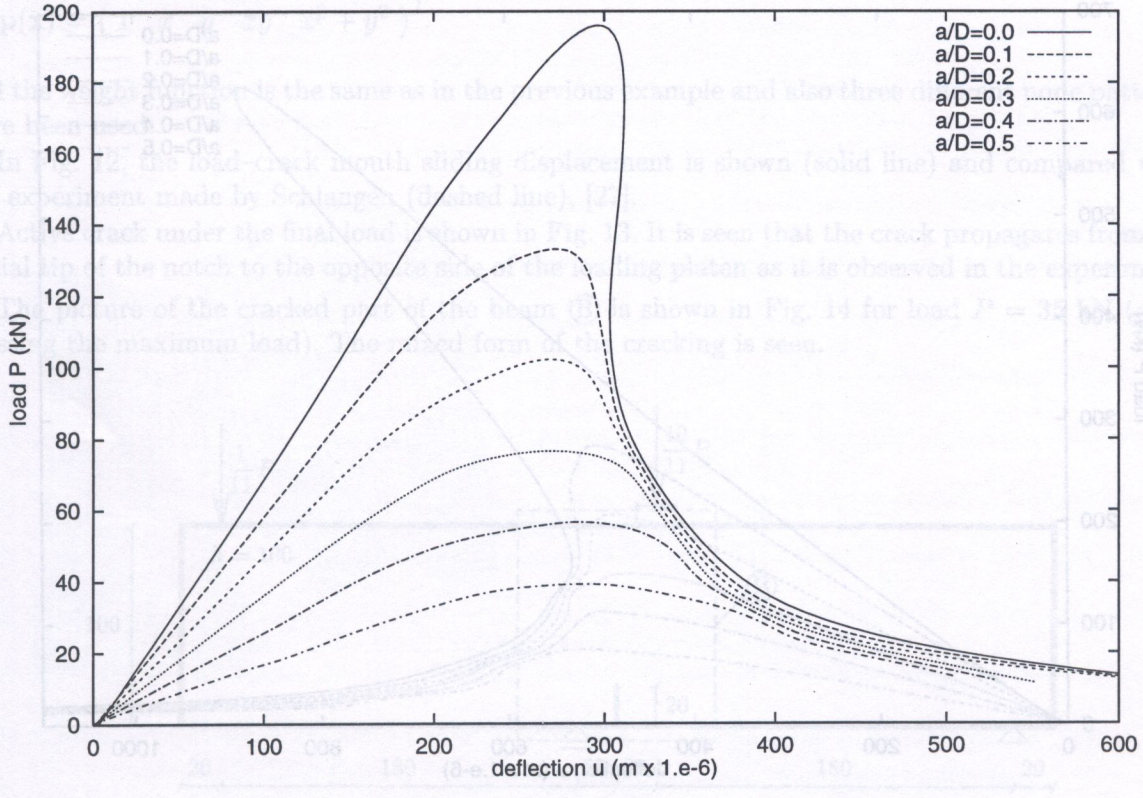

Fig. 7. Structural load–deflection response for $D = 1.6$ m

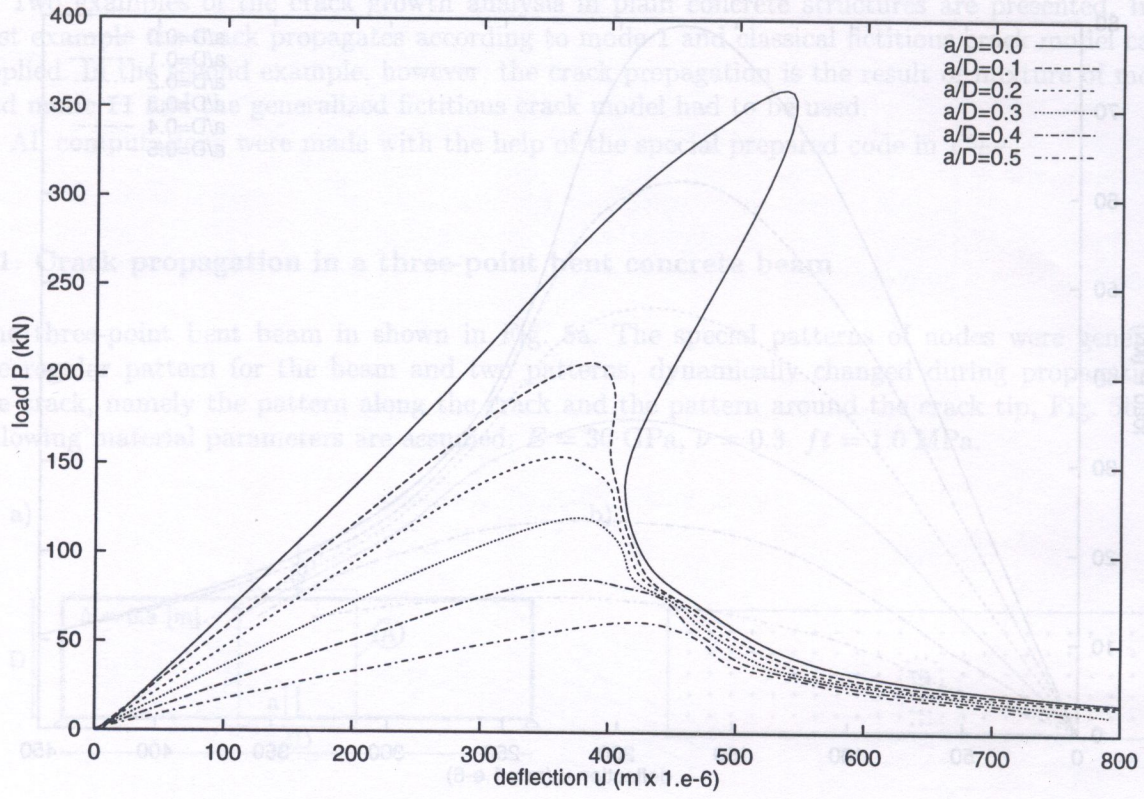

Fig. 8. Structural load–deflection response for $D = 3.2$ m

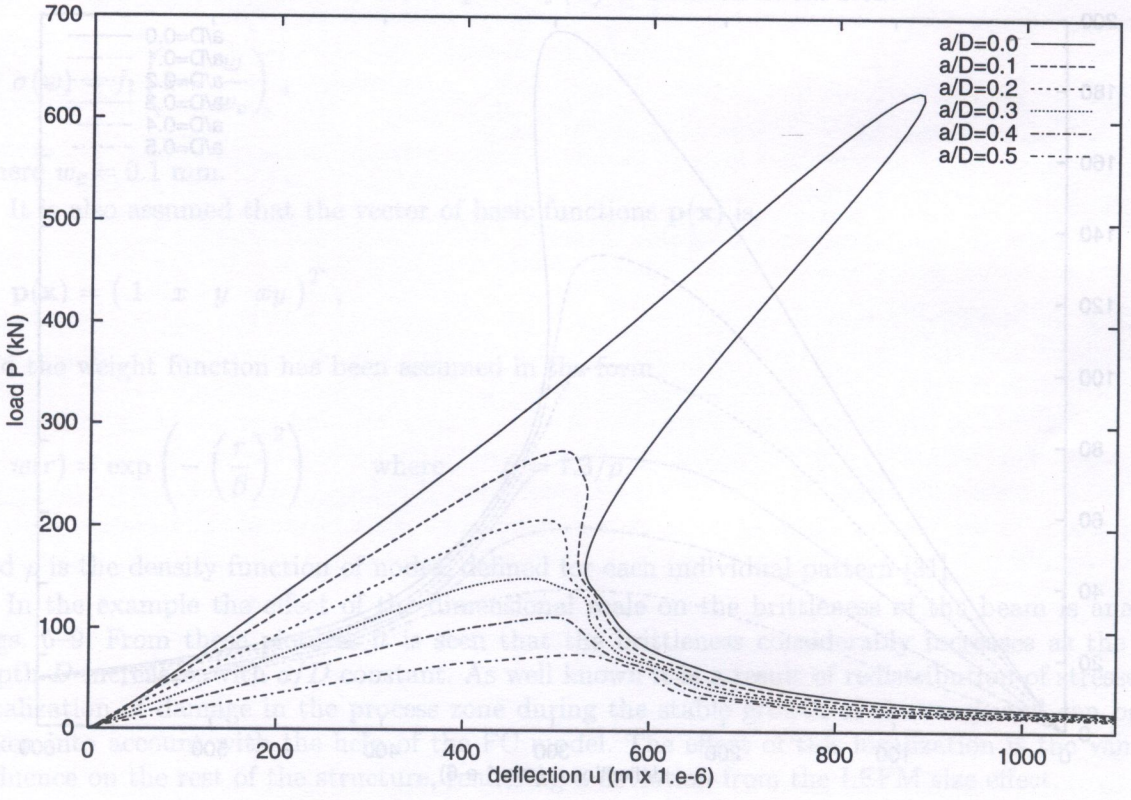

Fig. 9. Structural load–deflection response for $D = 6.4$ m

Fig. 10. Picture of the cracked three-point bend beam part Ⓐ

6.2. Iosipescu single-edge-notched concrete beam

The beam is shown in Fig. 11. The objective of the analysis is the application of the generalized fictitious crack model to simulate the mixture of the opening mode I and sliding mode II crack propagation. The following material parameters are assumed: $E = 35$ GPa, $\nu = 0.15$, $f_t = 2.8$ MPa [12].

The relationship $\sigma = f(w)$ in this example is of the expotential form,

$$\sigma(w) = f_t \exp\left(-\frac{10\,w}{w_c}\right), \tag{26}$$

where $w_c = 0.025$ mm has been calculated assuming that the fracture energy $G_f = 70$ Nm/m^2.

The vector of basic functions is assumed in the form

$$\mathbf{p}(\mathbf{x}) = \begin{pmatrix} 1 & x & y & xy & x^2+y^2 \end{pmatrix}^T \tag{27}$$

and the weight function is the same as in the previous example and also three different node patterns have been used.

In Fig. 12, the load–crack mouth sliding displacement is shown (solid line) and compared with the experiment made by Schlangen (dashed line), [27].

Active crack under the final load is shown in Fig. 13. It is seen that the crack propagates from the initial tip of the notch to the opposite side of the loading platen as it is observed in the experiment.

The picture of the cracked part of the beam Ⓑ is shown in Fig. 14 for load $P = 35$ kN (after crossing the maximum load). The mixed form of the cracking is seen.

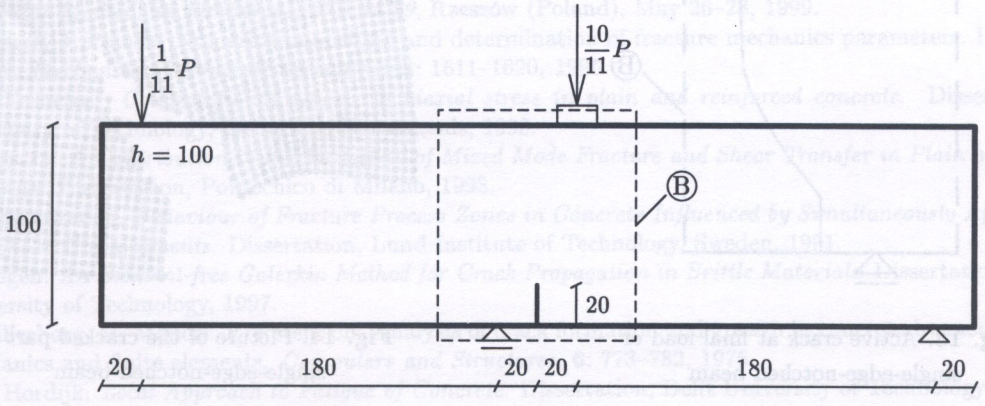

Fig. 11. Single-edge-notched beam; measures in [mm]

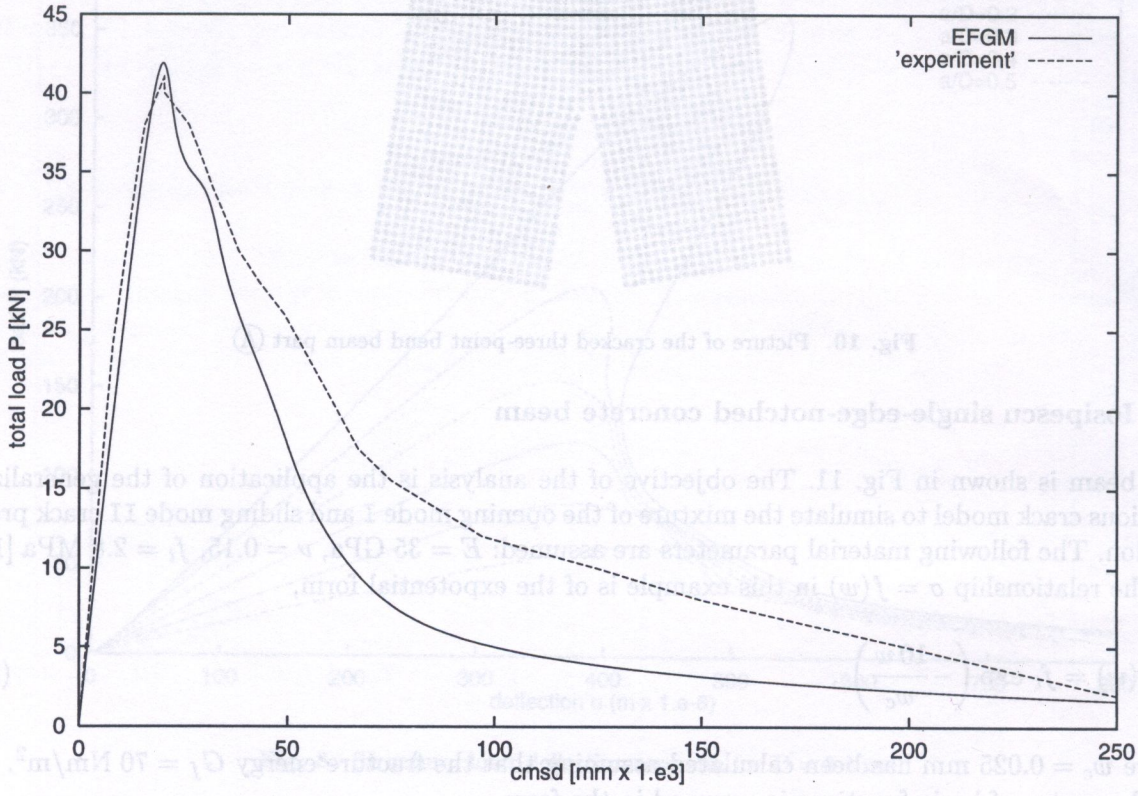

Fig. 12. Load–cmsd diagram for single-edge-notched beam

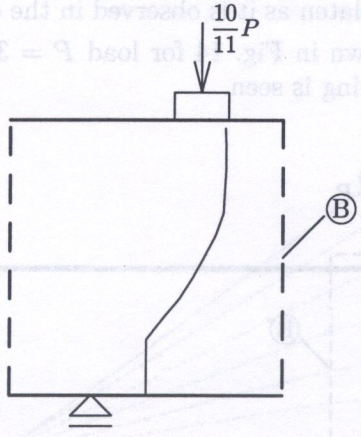

Fig. 13. Active crack at final load of single-edge-notched beam

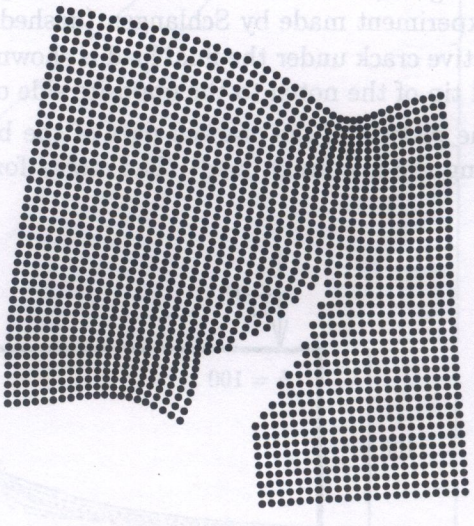

Fig. 14. Picture of the cracked part Ⓑ single-edge-notched beam

7. Conclusions

In the paper, an analysis of crack growth in quasi brittle materials like concrete is presented. The generalized fictitious crack model has been coupled to the Galerkin meshless method and the uniform algorithm of analysis worked out. It has been shown that, in spite of the elastic properties of material, a precise analysis needs iterative approach in order to obtain a state of equilibrium between external loads, cohesive forces and distribution of stresses, necessary for crack propagation to take place. In such an analysis, specially when the direction of the crack growth is unknown a priori, the effectiveness of the meshless method is obvious. As is well known, however, the disadvantages of these methods are mainly high computation time when compared to the finite element method. This is why in fracture mechanics coupling of the Galerkin meshless method to finite elements seems to be a very promising way of analysis. In this direction the algorithm of crack growth analysis presented in the paper is actually developed.

Acknowledgements

The support of the Polish Committee of Scientific Research in the frame of Grant No. 7T07A040415 is gratefully acknowledged.

References

[1] F. Barpi, S. Valente. Crack propagation under constant load: Constitutive laws for the process zone. In: de Borst, Bićanić, Mang, Meschke, eds., *Computational Modelling of Concrete Structures*, Balkema, Rotterdam, 1998.

[2] Z.P. Bazant, B.P. Oh. Crack band theory for fracture of concrete. *Materials and Structures*, **16**(93): 155–177, 1983.

[3] Z.P. Bazant, P.A. Pfeiffer. Determination of fracture energy from size effect and brittleness number. *ACJ Materials Journal*, **846**: 463–480, 1987.

[4] T. Belytschko, Y. Krongauz, M. Fleming, D. Organ, P. Krysl. Meshless methods: an overview and recent developments. *Computer Methods in Applied Mechanics Engineering*, **139**: 3–47, 1996.

[5] T. Belytschko, Y. Krongauz, M. Fleming, D. Organ, W.K. Liu. Smoothing and accelerated computations in the element free Galerkin method. *Journal of Computational and Applied Mathematics*, **74**: 111–126, 1996.

[6] T. Belytschko, Y.Y. Lu, L. Gu. Element-free Galerkin methods. *International Journal for Numerical Methods in Engineering*, **37**: 229–256, 1994.

[7] T. Belytschko, D. Organ, Y. Kronganz. A coupled finite element-free Galerkin method. *Computational Mechanics*, **17**: 186–195, 1995.

[8] I. Carol, P.C. Prat, C.M. Lopez. Normal shear cracking model: application to discrete crack analysis. *ASCE Journal of Engineering Mechanics*, 123(8), 1997.

[9] Al. Carpinteri, S. Valente, G. Ferrara, G. Melchiorri. Is mode II fracture energy a real material property? *Computers and Structures*, **48**(3): 397–413, 1993.

[10] C. Cichoń, J. Jaśkowiec. EFGM analysis of crack growth in quasi-brittle materials. In: *Polish Conference on Computer Methods in Mechanics, PCCM'99*, Rzeszów (Poland), May 26–28, 1999.

[11] M. Elices, J. Planas. Numerical modelling and determination of fracture mechanics parameters. Hilleborg type modes. *Mechanics of Concrete Structures*, **3**: 1611–1620, 1996.

[12] P.H. Feenstra. *Computational aspects of biaxial stress in plain and reinforced concrete.* Dissertation, Delft University of Technology, Delft, The Netherlands, 1993.

[13] L. Ferrara. *A Contribution to the Modelling of Mixed Mode Fracture and Shear Transfer in Plain and Reinforced Concrete.* Dissertation, Politecnico di Milano, 1998.

[14] M. Hassanzadeh. *Behaviour of Fracture Process Zones in Concrete Influenced by Simultaneously Applied Normal and Shear Displacements.* Dissertation, Lund Institute of Technology, Sweden, 1991.

[15] D. Hegen. *An Element-free Galerkin Method for Crack Propagation in Brittle Materials.* Dissertation, Eindhoven University of Technology, 1997.

[16] A. Hillerborg, M. Modeer, E. Petersson. Analysis of crack formation and growth in concrete by means of fracture mechanics and finite elements. *Computers and Structures*, **6**: 773–782, 1976.

[17] D.A. Hordijk. *Local Approach to Fatigue of Concrete.* Dissertation, Delft University of Technology, The Netherlands, 1991.

[18] B.L. Karihaloo. *Fracture Mechanics and Structural Concrete.* Longman, 1997.

[19] P. Lancaster, K. Salkauskas. Surface generated by moving least squares methods. *Mathematics and Computation*, **37**(155): 141–158, 1981.
[20] J. Lemaitre. *A Course on Damage Mechanics*. Springer Verlag, 1992.
[21] T. Liszka, J. Orkisz. The finite difference method at arbitrary irregular grids and its application in applied mechanics. *Computers and Structures*, **11**: 83–95, 1980.
[22] B. Nayroles, G. Touzot, P. Villan. Generalizing the finite element method: Diffuse approximation and diffuse elements. *Computational Mechanics*, **10**: 307–318, 1992.
[23] M.B. Nooru-Mohammed. *Mixed-mode fracture of concrete: an experimental approach*. Dissertation, Delft University of Technology, The Netherlands, 1992.
[24] U. Ohlsson, T. Olofsson. Mixed-mode fracture and anchor bolts in concrete analysis with inner softening bands. *Journal of Engineering Mechanics*, pages 1027–1033, 1997.
[25] J. Orkisz. Finite difference method. In: M. Kleiber, ed., *Handbook of Computational Solid Mechanics*, Chapter III, pp. 336–432. Springer-Verlag, Berlin, 1998.
[26] G. Pijaudier-Cabot, Ch. La Bordiere, S. Fichant. Damage mechanics for concrete modelling: applications and comparisons with plasticity and fracture mechanics. In: *International Conference EURO-1994*, vol. 1, pages 17–36, 1994.
[27] E. Schlangen. *Experimental and Numerical Analysis of Fracture Process in Concrete*. Dissertation, Delft University of Technology, The Netherlands, 1993.
[28] M. van Gils. *Quasi-Brittle Fracture of Ceramics*. Dissertation, Eindhoven University of Technology, 1997.
[29] J.G.M van Mier. *Fracture Process of Concrete*. CRC Press, 1997.
[30] P. Wawrzynek, A.R. Ingraffea. *Discrete Modelling of Crack Propagation. Theoretical Aspects and Implementation Issues in Two and Three Dimensions*. Report 91-5, School of Civil and Environmental Engineering, Cornell University, Ithaca, 1991.
[31] G. Yagawa, T. Yamada. Free mesh method: A kind of meshless finite element method. *International Journal of Computational Mechanics*, **9**: 333–346, 1992.